Optical Materials xxx (2016) xxx-xxx

Contents lists available at ScienceDirect

Optical Materials

journal homepage: www.elsevier.com

Second-order nonlinear optical properties of mexylaminotriazine-functionalized glass-forming azobenzene derivatives

Hirohito Umezawa [a, b, 1], Matthew Jackson [a], Olivier Lebel [c], Jean-Michel Nunzi [b, d], Ribal Georges Sabat [a, *]

[a] Department of Physics, Royal Military College of Canada, Kingston, Ontario K7K7B4, Canada
[b] Department of Chemistry, Queen's University, Kingston, Ontario K7L3N6, Canada
[c] Department of Chemistry and Chemical Engineering, Royal Military College of Canada, Kingston, Ontario K7K7B4, Canada
[d] Department of Physics and Engineering Physics and Astronomy, Queen's University, Kingston, Ontario K7L3N6, Canada

ARTICLE INFO

Article history:
Received 17 May 2016
Received in revised form 4 July 2016
Accepted 27 July 2016
Available online xxx

Keywords:
Azobenzene materials
Optical nonlinearities in organic materials
Second harmonic generation
Nonlinear optics
Optical properties of thin films
Second order susceptibility coefficients

ABSTRACT

The second-order nonlinear optical coefficients of thin films of mexylaminotriazine-functionalized azobenzene molecular glass derivatives were measured using second harmonic generation. The thin films were poled using a custom corona poling set-up and the second harmonic light from a pulsed 1064-nm laser was detected. Four out of the six tested compounds showed optical nonlinearity and a maximum coefficient of 75 pm/V was obtained. The time dependence of the nonlinear coefficients was studied under ambient light and under dark; the second harmonic generation intensity stayed constant for thiazole-containing derivatives while a significant decay was measured for the other compounds.

1. Introduction

Organic nonlinear optical materials are developed for their compatibility with microelectronics and integrated optical technologies where they have been used in a multitude of applications ranging from optical signal modulators [1] to sensors and imaging devices [2]. Nonlinear optical behavior in amorphous organic materials is only realized by permanently reorienting the molecules in order to create an asymmetry in the material [3]. This is typically achieved by heating the material above its glass transition temperature (T_g) to achieve higher molecular mobility, and subsequently applying either a contact or corona poling electric field for a period of time, followed by cooling the material to room temperature with the electric field still being applied [4,5]. The contact poling technique requires the electric field to be applied directly onto the material while the corona field is the result of a partial breakdown of air causing accumulation of charges at the material's surface. Corona poling is advantageous over contact poling because the later has an increased chance of arcing through the electrodes with a possible destruction of the poled material as a result. However, both methods rely on the permanent dipole moment of the molecules being large enough.

Polymers have been prevalent in organic nonlinear optics not only because they exhibit high optical damage threshold and a substantial ease of processing and manufacturing compared to inorganic materials, but also because their optical, structural and mechanical properties can be tailored to suit any particular application [6]. Moreover, polymeric systems typically possess low dielectric permittivity, which is essential for fast-switching optical devices and they have been proven to show electro-optic coefficients similar to the most commonly used inorganic nonlinear optical materials.

Azobenzene-containing polymers are well known for their remarkable ability to reversibly photoisomerize between the *trans* and *cis* configurations upon irradiation with an absorbing laser wavelength. Consequently, upon exposure to an interfering laser beam, surface relief nanogratings appear in azo polymer thin films due to the mass molecular migration from high irradiance to low irradiance zones [7]. Aside from their molecular photo-switching abilities, both azo polymers [8] and hyperbranched azo polymers [9,10] have been studied for their photoinduced birefringence and optical nonlinearities for use in optical data storage and processing applications [11]. Electro-optic modulation [12], second harmonic [13], and even third harmonic [14] generation of light have been studied in azo polymers using both corona poling and all-optical poling setups [15], where, in the latter, partial molecular reorientation is achieved uniquely with light.

On the other hand, organic glasses offer a new processing technology, which combines both the advantages of polymers (wet processing of glassy materials, multi-functionalization and self-organization)

* Corresponding author.
Email address: sabat@rmc.ca (R.G. Sabat)
[1] Current address: Department of Chemistry and Biochemistry, National Institute of Technology, Fukushima College, Iwaki, Fukushima 970-8034, Japan.

http://dx.doi.org/10.1016/j.optmat.2016.07.037
0925-3467/

and the advantages of small molecules (ease of synthesis, reproducibility, high uniformity and high density of active functions). Recently, our group synthesized mexylaminotriazine-substituted azobenzene molecular glass **4**, with nearly identical photomechanical properties to azo polymers, but with the added benefit of easier synthesis and higher yield [16]. Moreover, we recently synthesized closely related molecular glasses (**1**–**3** and **5**–**6**) containing azobenzene chromophores with various absorption maxima [17]. All the aforementioned compounds, represented in Fig. 1, form high quality amorphous films with strong resistance to crystallization. We have previously shown that the photomechanical properties for this series of azobenzene-functionalized molecular glasses vary significantly from one compound to another, and were found to be highly dependent on the chromophore [17]. In this work, these same compounds have been renumbered sequentially with increasing maximum absorption wavelength and their second-order nonlinear properties were probed.

2. Experimental section

Thin films of compounds **1**–**6** were corona-poled and tested for the generation of second harmonic light using a pulsed 1064-nm laser. It was found that only compounds **3**–**6** exhibited second-order nonlinear optical properties, despite the fact that some of these compounds previously showed very weak photomechanical properties [17]. The second-order nonlinear optical coefficients, d_{31}, d_{15} and d_{33}, of compounds **3**–**6** were measured using the Maker fringe method [18]. Both the optical absorbance of the films and their nonlinear behavior seemed to change as a function of the poling temperature. Furthermore, the time dependence of the second harmonic signals was measured for compounds **3**–**6** and a significant difference was found in the test samples stored under ambient light compared to those stored under dark. Finally, in order to calculate the second-order nonlinear optical coefficients, the refractive indices of thin films of compound **4** were determined experimentally as a function of wavelength by waveguiding a light beam through them using a laser-inscribed diffraction grating.

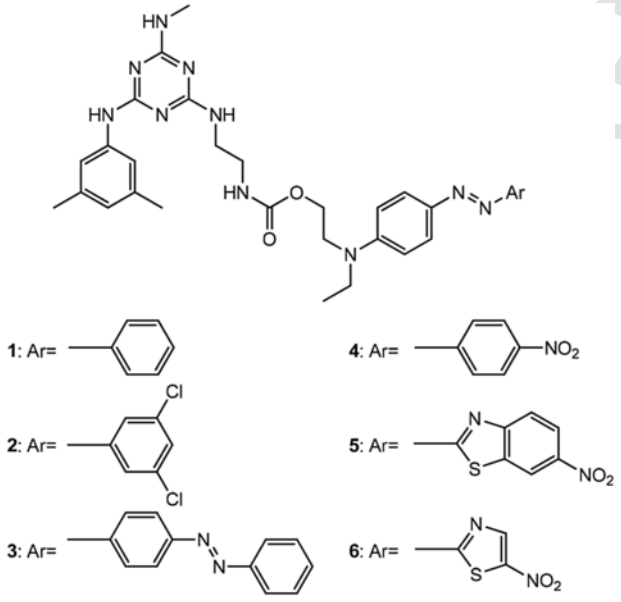

Fig. 1. Molecular structures of azobenzene-functionalized molecular glass derivatives **1**–**6**.

2.1. Experimental set-up

A New Wave Research (Polaris II 20 Hz) pulsed Nd:YAG 1064-nm laser with a maximum energy of 50 mJ with 7 ns pulses was used for this experiment. As depicted in Fig. 2, the laser light passed through a half-wave plate followed by a linear polarizer and a long pass filter to remove any residual 532-nm light originating from the laser cavity and the half-wave plate. The laser beam was then focused using a converging lens to increase the localized irradiance onto the sample, which was mounted to a computer-controlled rotational stage. After passing through the sample, the laser light went through a harmonic beam splitter and continued through to a beam stop. The generated second harmonic light was reflected and directed towards a prism to eliminate stray 1064-nm light and then sent through another polarizer, focusing lens, short pass filter, and finally an interference filter before reaching a silicon photodiode. Finally, the signal from the photodiode was recorded on a computer using a Labview program.

2.2. Thin film preparation

Compounds **1**–**6** were dissolved in CH_2Cl_2 to yield solutions with a concentration of 4 wt%. The solutions were then mechanically stirred for 1 h before being filtered through a 0.45 μm syringe filter. Thin film deposition was performed using a Headway Research spin-coater. Each thin film consisted of approximately 0.2 mL of solution spread across a 3×3 cm^2 cleaned and dried BK7 glass slide. After deposition, each slide was spun at a rate of 1000 rpm for 20 s to ensure a uniform spread. The films were then dried in a Yamato ADP-21 oven at 95 °C for 30 min. The final product was a uniform thin film with an average thickness of approximately 400 nm, as measured using a Sloan Dektak II D profilometer (model 139961).

2.3. Electric-field poling

Molecular re-alignment of thin films made of compounds **1**–**6** was performed using a custom-built corona poling station. This apparatus used a Cole-Parmer Digi-Sense temperature controller to heat an alu-

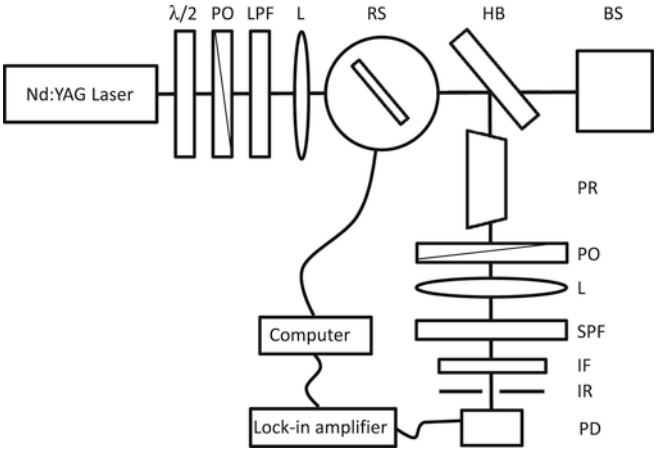

Fig. 2. Experimental setup for SHG measurements: λ/2 – half-wave plate, PO – linear polarizer, LPF – long pass filter, L – lens, RS – rotational stage, HB – harmonic beam splitter, BS – beam stop, PR – prism, SPF – short pass filter, IF – interference filter, IR – iris, PD – photodiode.

minum hot plate, with a 5-cm radius, up to 100 °C. Each sample was placed onto the hot plate and its temperature was monitored using a calibrated P-N junction temperature sensor directly connected to the temperature controller. The hot plate itself acted as one of the electrodes with a thin metallic wire as the second electrode, which was held horizontally at 0.9 cm above the hot plate using a hollow 7.5-cm round aluminum tube. The corona discharge voltage was supplied by a Hippotronics High-Voltage DC power supply and the current was monitored using a Fluke multimeter. After heating, the sample and poling fixture were cooled down to room temperature using a fan.

2.4. DFT calculations

The geometries of N,N'-dimethylamino analogues of the azo chromophores of compounds **1**–**6** in the *trans* configuration were optimized using Density Functional Theory (DFT) calculations (B3LYP/6-31G(d)) with the Wavefunction Spartan 06 software. Dipole moments were given in the calculation output.

3. Results and analysis

The generation of second harmonic signals was tested for thin films of compounds **1**–**6**. The T_g of these compounds varies between 63 °C and 73 °C [17]. So, in order to achieve the most complete reorientation of the molecules, corona poling was performed at temperatures ranging from 60 °C to 100 °C with a constant voltage of 8 kV, applied for times up to 30 min Fig. 3(a) shows a decrease in absorbance of thin films of compound **5**, as a function of poling temperature for a time of 20 min. This decrease in absorbance was observed for all compounds **1**–**6**, and is to be expected since molecular rearrangement leads to a higher transparency of the samples. This is also related to the typical decrease in the film's refractive index after poling and the slight shift in the maximum absorbance wavelength due to the DC Stark effect [3], which can also be seen in Fig. 3(a).

The second harmonic generation (SHG) signal intensity from thin films of compound **5** was measured as a function of the laser incidence angle for films poled at different temperatures, as shown in Fig. 3(b). A significant increase can be observed in the SHG signal for the films poled at 90 °C and 100 °C compared to the film poled at 80 °C for compound **5**. Even though the absorbance decreased for films poled at 100 °C in comparison to films poled at 90 °C, no corresponding increase in SHG intensity was recorded. This is possibly due to the degradation of samples poled at 100 °C. Therefore, it was concluded that the maximum optical nonlinearity was achieved for compound **5** at a poling temperature of 90 °C and all subsequent films made with this compound were poled at this temperature. Similar tests for films of compound **6** were done and a similar maximum poling temperature of 90 °C was obtained. Furthermore, identical tests for films of compounds **3**–**4** were done and a maximum respective poling temperature of 60 °C and 65 °C were measured. At higher poling temperatures, the samples of compounds **3**–**4** lost optical clarity, developing a scattering aspect. Even after poling at various temperatures and times while retaining optical clarity, films of compounds **1**–**2** did not show any SHG signal. It is believed that the reason for this behavior is related to the dipole moment of the respective azo chromophores. The poling process is known to result in the alignment of the dipoles of the chromophores, and the alignment rate during poling is proportional to the dipole moment of the azo moieties. The dipole moments of model azo compounds analogous to the chromophores of compounds **1**–**6** were calculated using DFT calculations, and are listed in Table 1. Chromophores without both a strong electron donor and acceptor group will show less electron delocalization by resonance (push-pull effect), thereby yielding lower first order hyperpolarizability and permanent dipole moment. Low dipole moment tends to yield a lower degree of alignment, providing a rationale why compounds **1**–**2** failed to give any measurable SHG signal, while compound **5**, which shows the highest dipole moment, gives the highest SHG signal. One notable exception to this trend is compound **3**, which shows a smaller dipole moment than compound **2**. However, in this case, the dipole moment calculation takes into account the two chloride atoms of compound **2**, which are not conjugated with the azo chromophore, and therefore do not contribute to the resonance, which regulates several physical properties of azo chromophores, including absorption range, rates of *cis-trans* isomerization and most importantly the first order hyperpolarizability, which is expected to increase with conjugation length.

The experimental setup illustrated in Fig. 2 allowed varying the incident laser light polarization, as well as the polarization of the measured SHG signal. This was done in order to obtain the various second-order nonlinear optical coefficients in the d_{ij} tensor. Fig. 4 shows the angular dependence of the SHG intensity from films of compound **4** using various combinations of incident light and SHG light polarizations, in order to calculate the d_{31}, d_{15} and d_{33} coefficients. In this figure, the "p-in", "s-in" and "45°-in" refer to the inci-

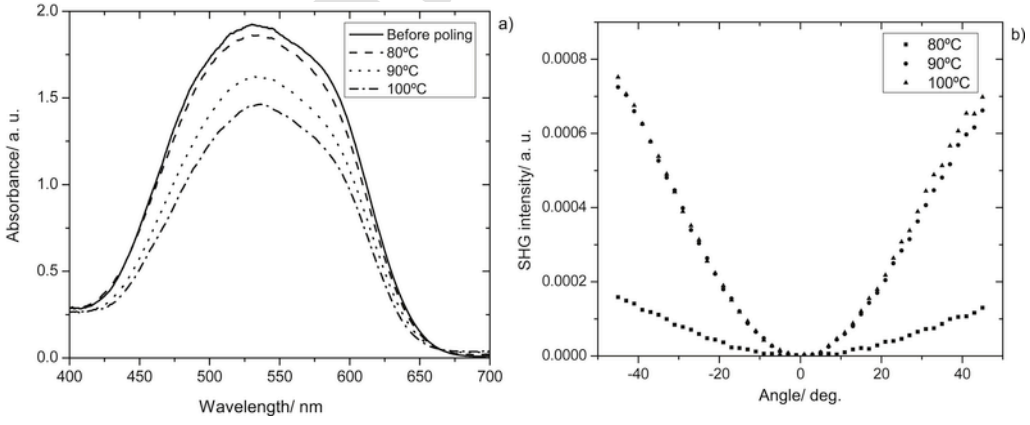

Fig. 3. Temperature dependence of compound **5** after corona poling under a voltage of 8 kV for 20 min a) visible absorption spectrum and b) incidence angle dependence of p-polarized SHG intensity.

Table 1
Dipole moments of azo chromophores **1**–**6**, calculated by DFT (B3LYP/6-31G(d)).

Compound	Dipole moment (D)
1	4.11
2	7.55
3	5.26
4	11.12
5	13.07
6	12.47

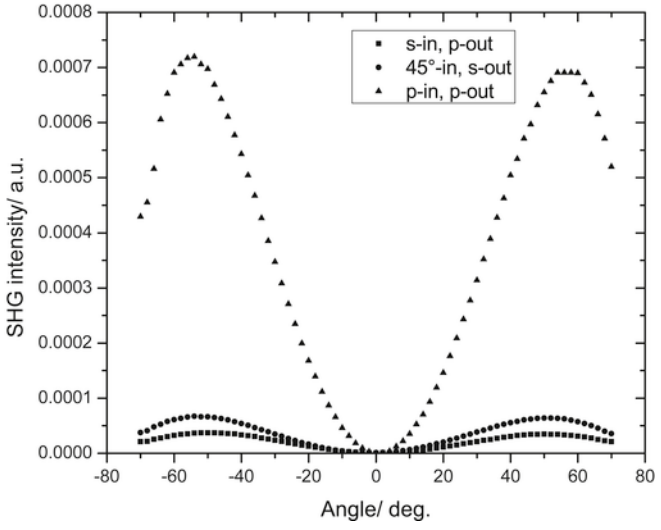

Fig. 4. SHG signal intensity as a function of angle for films of compound **4**.

dent laser beam polarization, while "p-out" and "s-out" refer to the polarization of SHG light measured with the photodiode.

For calculating the d_{31}, d_{15} and d_{33} coefficients, the refractive index of the films needed to be measured both at 1064 nm and 532 nm. Since surface relief diffraction gratings (SRG) could be inscribed on thin films of compound **4**, coupled mode waveguiding theory was used to find the refractive indices of the films at various wavelengths. Several identical films of compound **4** were prepared and SRGs were laser-inscribed on each of those films, having an average thickness of 415 nm. The gratings were inscribed with pitches varying between 350 nm and 800 nm. A scanning monochromator was then used to measure the reflection intensity plots as a function of wavelength for each SRG. Coupling of resonant waves inside each film were seen as negative peaks in the reflection plots. The films were thin enough to only allow the propagation of one resonant mode at a particular incident light polarization. The wavelength of light, which propagates through the film, is dependent on several parameters including the refractive indices of the cladding (air), the film and the substrate, the incidence angle of light, the light polarization and the grating pitch. In this experiment, only the grating pitch was varied and this yielded coupling wavelengths measured between 615 nm and 1222 nm. Subsequently, the transcendental equation for mode propagation was numerically solved using computational software in order to obtain the film's refractive index at the light-coupling wavelength [19]. The refractive index dispersion plot of thin films of compound **4** was obtained and is shown in Fig. 5.

The following Sellmeier equation [20] was fitted to the experimental data and the refractive index parameters were found, as seen

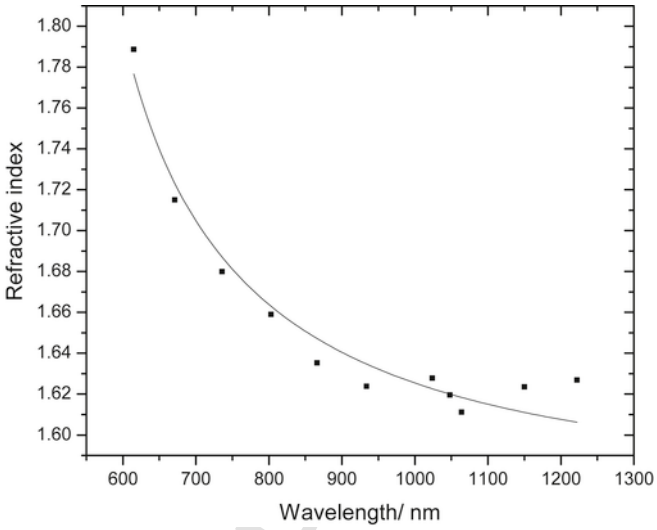

Fig. 5. Dispersion curve for thin films of compound **4** fitted to Sellmeier's equation.

in Table 2.

$$n^2 = 1 + \frac{A_1\lambda^2}{\lambda^2 - B_1} + \frac{A_2\lambda^2}{\lambda^2 - B_2} \tag{1}$$

Using the parameters in Table 2 and Eq. (1), the refractive indices of the sample films were calculated at 1064 nm (n_s^{ω}) and at 532 nm ($n_s^{2\omega}$) and they were found to be respectively 1.62 and 2.02. It was estimated that films of the other compounds showed closely similar refractive indices.

The thickness of the films was too small to show a typical Maker fringe pattern. The maximum SHG intensity was verified to be at the nonlinear Brewster angle [21] and the second-order nonlinear optical coefficients were obtained using the following equation [22,23]:

$$\frac{d_{eff}}{d_q} = \frac{2L_{qc}\sqrt{T_q}n_s^{\omega}\sqrt{n_s^{2\omega}}\cos\left(\theta_s^{\omega}\right)\sqrt{I_s^{2\omega}/I_q^{2\omega}}}{\pi L_s \mathrm{sinhc}\left(\alpha L_s/2\right)\exp\left(-\alpha L_s/2\right)n_q^{\omega}\sqrt{n_q^{2\omega}}\sqrt{T_s}} \tag{2}$$

where d_{eff} is the effective second-order nonlinear optical coefficient, which depends on the polarizers configuration, d_q is the nonlinear coefficient of a reference *Y*-cut quartz crystal ($d_q = d_{11} = 0.45$ pm/V [24]), L_{qc} is the coherence length of the quartz (calculated to be 20.6 μm), T_q is the transmittance of the quartz (calculated to be 0.8711), θ_s^{ω} is the light incidence angle inside a test sample at the

Table 2
Sellmeier's refractive index parameters from Eq. (1).

Parameter	Value
A_1	0.23835
A_2	1.2342
B_1	0.23523 μm^2
B_2	7.2361×10^{-2} μm^2

maximum SHG signal and calculated at the first harmonic frequency, L_s is the sample thickness, αL_s is the sample's optical depth ($\alpha L_s = A \ \ln \ 10$, where A is the absorbance at 532 nm), T_s is the sample's transmittance and finally, I_q^{ω} and $I_q^{2\omega}$ are the SHG signal intensities of the sample and the quartz respectively.

The nonlinear coefficients of each test sample was calculated from the d_{eff} value in Eq. (2), using the following equations:

$$d_{31} = d_{eff} / \sin\left(\theta_s^{2\omega}\right) \tag{3}$$

Table 3
Second-order nonlinear coefficients of compounds **3**–**6**.

Films	d_{31} pm.V^{-1}	d_{15} pm.V^{-1}	d_{33} pm.V^{-1}
3	19 ± 1	17 ± 1	59 ± 15
4	30 ± 2	31 ± 2	75 ± 27
5	35 ± 2	34 ± 2	46 ± 26
6	27 ± 2	18 ± 1	50 ± 15

$$d_{15} = d_{eff} / \sin\left(\theta_s^{\omega}\right) \tag{4}$$

$$d_{33} = \frac{d_{eff} - 2d_{15}\ \sin\left(\theta_s^{\omega}\right)\cos\left(\theta_s^{\omega}\right)\cos\left(\theta_s^{2\omega}\right) - d_{31}\cos^2\left(\theta_s^{\omega}\right)\sin}{\sin^2\left(\theta_s^{\omega}\right)\sin\left(\theta_s^{2\omega}\right)}$$

Table 3 shows the calculated values of d_{31}, d_{15} and d_{33} for thin films of compounds **3**–**6**.

The time dependence of the SHG signal intensity was measured for a maximum time of 180 h. The normalized d_{eff} is given by the ratio of $\sqrt{I_s^{2\omega}}$ for a certain time over $\sqrt{I_s^{2\omega}}$ at time equals zero, according to Eq. (2). This was done in order to study the long-term stability of the poled nonlinear films of compounds **3**–**6**, since this is necessary for practical applications. All the test samples were fabricated and poled under the same conditions as previously. Moreover, some samples were kept under ambient light while others were kept under complete darkness, immediately after poling was complete. As seen in Fig. 6, compound **3** showed the most significant decrease in its optical nonlinearity compared to the other compounds. Also, compounds **3**–**4** showed a considerable decrease in their normalized d_{eff} coefficient for samples kept under ambient light compared to samples kept under dark. On the other hand, samples of compound **5** showed almost no decline in performance when kept under either light or

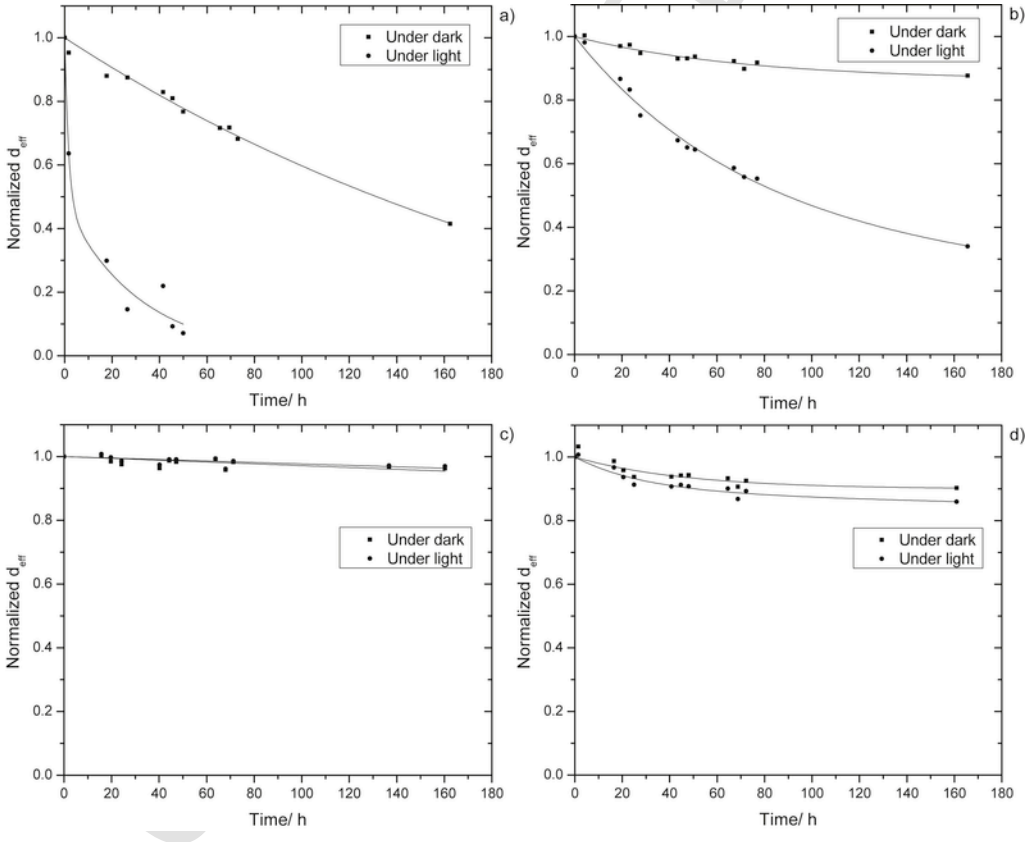

Fig. 6. Time dependence of the normalized d_{eff} of thin films of (a) compound **3** (b) compound **4** (c) compound **5** and (d) compound **6**.

dark conditions, while compound **6** films exhibited only a small decrease (less than 10%).

Interestingly, our study shows that orientation stability of a poled molecular glass, namely compound **5**, is larger than the stability of poled PMMA-based nonlinear polymers, despite the larger entanglement offered by polymers [11]. Also, the azothiazole chromophores from compounds **5**–**6** show a much higher stability of SHG compared to classic azobenzene chromophores, such as those found in compounds **3**–**4**. The exact causes of this difference in stability are not yet well-understood, but azothiazole chromophores have higher dipole moments than their azobenzene analogues, especially when substituted with nitro groups [25,26]. One consequence of these stronger dipoles is a slower *cis-trans* isomerization process [27], as was witnessed by their inability to easily form SRGs [17]. Additionally, this would lead to the presence of stronger dipole-dipole intermolecular interactions between azo moieties in the bulk material. Stronger dipoles may thus contribute to limit molecular mobility in the films, both from an intramolecular and from an intermolecular standpoint. Furthermore, the nitrogen atom within the thiazole ring can act as a hydrogen bond acceptor, and can form hydrogen bonds with the N-H groups from the glass-forming triazine units, thereby reinforcing molecular cohesion in the solid [28].

4. Conclusion

Six different mexylaminotriazine-functionalized azobenzene molecular glass derivatives were corona poled at temperatures ranging from 60 °C to 100 °C. Using a pulsed 1064-nm Nd:YAG laser, second harmonic light was generated in thin films made from these compounds and the second-order nonlinear optical coefficients d_{31}, d_{15}, and d_{33} were obtained using the Maker fringe method. Despite the various temperatures used for the corona poling process, only compounds **3**–**6** demonstrated measurable second-order nonlinear properties and a maximum d_{33} coefficient of 75 pm/V was obtained for compound **4**. In addition to their first order hyperpolazizability, it is understood that the ability of the different compounds to show a nonlinear optical behavior under corona poling is related to the strength of the molecules' dipole moment for each respective azo chromophore, which is correlated to electron delocalization by resonance, as it was calculated using DFT simulations. Compounds **1**–**2**, which do not possess a strong electron acceptor group, do not show any nonlinear optical properties as a result. Upon measuring the time dependence of the nonlinear coefficients, a significant decrease was observed for compounds **3** and **4** for samples stored under ambient room light compared to samples stored under dark. Thin films of compound **5** showed the best long term performance while films of compound **6** had only a slight performance decrease.

Acknowledgement

The authors would like to acknowledge research funding from the Canadian Defense Academy Academic Research Program (OL), Natural Sciences and Engineering Research Council of Canada (RGPIN-2015-05743 for RGS and RGPIN-2015-05485 for JMN).

References

[1] G. Xu, Z. Liu, J. Ma, B. Liu, S. Ho, L. Wang, P. Zhu, T.J. Marks, J. Luo, A.K.Y. Jen, Opt. Exp. 13 (2005) 7380–7385.
[2] S.R. Marder, Chem. Commun. (2006) 131–134.
[3] F. Kajzar, J.-M. Nunzi, Molecular orientation techniques, in: F. Kajzar, R. Reinisch (Eds.), Beam Shaping and Control with Nonlinear Optics, Kluwer academic publishers, New York, 1998, pp. 101–132.
[4] M. Eich, A. Sen, H. Looser, G.C. Bjorklund, J.D. Swalen, R. Twieg, D.Y. Yoon, J. Appl. Phys. 66 (1989) 2559–2567.
[5] R.A. Hill, A. Knoesen, M.A. Mortazavi, Appl. Phys. Lett. 65 (1994) 1733–1735.
[6] R.G. Tasaganva, M.Y. Kariduraganavar, R.R. Kamble, S.R. Inamdar, Synth. Met. 161 (2011) 1787–1799.
[7] P. Rochon, E. Batalla, A. Natansohn, Appl. Phys. Lett. 66 (1995) 136–138.
[8] F.J. Rodriguez, C. Sanchez, B. Villacampa, R. Alcalà, R. Cases, M. Millaruelo, L. Oriol, Polymer 45 (2004) 2341–2348.
[9] J. Xie, X. Deng, Z. Cao, Q. Shen, W. Zhang, W. Shi, Polymer 48 (2007) 5988–5993.
[10] Z. Li, A. Qin, J.W.Y. Lam, Y. Dong, Y. Dong, C. Ye, I.D. Williams, B.Z. Tang, Macromolecules 39 (2006) 1436–1442.
[11] S.K. Yesodha, C.K.S. Pillai, N. Tsutsumi, Prog. Polym. Sci. 29 (2004) 45–74.
[12] K.D. Singer, M.G. Kuzyk, W.R. Holland, J.E. Sohn, S.J. Lalama, R.B. Comizzoli, H.E. Katz, M.L. Schilling, Appl. Phys. Lett. 53 (1988) 1800–1802.
[13] Y. Wang, O.Y. Tai, C.H. Wang, J. Chem. Phys. 123 (2005) 164704.
[14] L. Brzozowski, E.H. Sargent, J. Mater. Sci. Mater. Electron 12 (2001) 483–489.
[15] W. Chalupczak, C. Fiorini, F. Charra, J.M. Nunzi, P. Raimond, Opt. Commun. 126 (1996) 103–107.
[16] R. Kirby, R.G. Sabat, J.M. Nunzi, O. Lebel, J. Mater. Chem. C 2 (2014) 841–847.
[17] O.R. Bennani, T.A. Al-Hujran, J.M. Nunzi, R.G. Sabat, O. Lebel, New J. Chem. 39 (2015) 9162–9170.
[18] P.D. Maker, R.W. Terhune, M. Nisenoff, C.M. Savage, Phys. Rev. Lett. 8 (1962) 21–22.
[19] R.J. Stockermans, P.L. Rochon, Appl. Opt. 38 (1999) 3714–3719.
[20] A. Sommerfeld, Optics: Lectures on Theoretical Physics, Academic Press, 1967.
[21] N. Bloembergen, P. Pershan, Phys. Rev. 128 (1962) 606–622.
[22] M.A. Mortazavi, B.G. Higgins, A. Dienes, A. Knoesen, S.T. Kowel, J. Opt. Soc. Am. B 6 (1989) 733–741.
[23] W.N. Herman, L.M. Hayden, JOSA B 12 (1995) 416–427.
[24] M.G. Kuzyk, C.W. Dirk, Characterization Techniques and Tabulations for Organic Nonlinear Optical Materials, first ed., Marcel Dekker, New York, 1998.
[25] L. Chen, Y. Cui, G. Qian, M. Wang, Dyes Pigments 73 (2007) 338–343.
[26] Y. Cui, G. Qian, L. Chen, Z. Wang, M. Wang, Dyes Pigments 77 (2008) 217–222.
[27] P. Rochon, J. Gosselin, A. Natansohn, S. Xie, Appl. Phys. Lett. 60 (1992) 4–5.
[28] A. Plante, D. Mauran, S.P. Carvalho, J.Y.S.D. Pagé, C. Pellerin, O. Lebel, J. Phys. Chem. B 113 (2009) 14884–14891.